Supporting Information

Well-structured Bimetallic Surface Capable of Molecular Recognition for Chemoselective Nitroarene Hydrogenation

Shinya Furukawa,* Katsuya Takahashi, and Takayuki Komatsu*

Department of Chemistry, Tokyo Institute of Technology, 2-12-1-E1-10 Ookayama, Meguro-ku, Tokyo 152-8551, Japan

Corresponding authors

Shinya Furukawa

Department of Chemistry, Graduate School of Science and Engineering, Tokyo Institute of Technology, 2-12-1-E1-10 Ookayama, Meguro-ku, Tokyo 152-8551, Japan

E-mail: *furukawa.s.af@m.titech.ac.jp,* Tel: +81-3-5734-2602, Fax: +81-3-5734-2758

Takayuki Komatsu

Department of Chemistry, Graduate School of Science and Engineering, Tokyo Institute of Technology, 2-12-1-E1-10 Ookayama, Meguro-ku, Tokyo 152-8551, Japan

E-mail: *komatsu.t.ad@m.titech.ac.jp,* Tel: +81-3-5734-3532, Fax: +81-3-5734-2758

Table S1. Surface energy (γ) and surface Rh–Rh coordination number in the first coordination sphere (N_{Rh}^{surf}) for various low index Miller Planes of Rh-based alloys.[a]

compound	space group	plane	γ / Nm^{-2}	N_{Rh}^{surf}	selected
RhZn	$Pm\bar{3}m$	(100)	2.36(14)	0	
		(110)	1.49	2	✓
		(111)	2.17(08)	0	
RhGa	$Pm\bar{3}m$	(100)	2.25(69)	0	
		(110)	1.11	2	✓
		(111)	1.72(40)	0	
RhIn	$Pm\bar{3}m$	(100)	2.15(36)	0	
		(110)	0.92	2	✓
		(111)	1.82(24)	0	
RhSn	$P2_13$	(210)	1.27	2	
		(012)	0.98	3	✓
		(211)	1.17	3	
RhPb	$P6/mmm$	(002)	1.12(14)	4	✓
		(201)	0.74	2	
		(211)	0.83	1	
RhBi	$P6_3/mmc$	(100)	2.94(42)	0	
		(102)	0.80	0	
		(110)	0.75	2	✓
$RhPb_2$	$I4/mcm$	(100)	0.84(03)	2	✓
		(001)	0.98(02)	0	
		(211)	0.49	1	

[a] Low-index Miller planes with low γ and high N_{Rh}^{surf} were selected as surfaces that were expected to be exposed and active for hydrogenation reactions and CO adsorption. [b] The number with parenthesis indicates the center value and the range (half width) of γ.

Table S2. Theoretical and experimental frequencies of CO adsorbed on various Rh-based planes.

site	surface		geometry	Vibrational frequency of adsorbed CO /cm^{-1}		
				theoretical [a] (this study)	experimental (this study)	experimental (literature)
atop	Rh	(111)	(3×3)	2019		2015[1]
			(2×2)	2032		
			($\sqrt{3}\times\sqrt{3}$)R30°	2046		2041[1]
			c(4×2)-2CO	2053	2057	
			(2×2)-3CO	2066		2070[1]
	RhIn	(100)	(2×2)	2010		
		(110)	(2×2)	2006	2002	
		(111)	(2×2)	1994		
	RhZn	(100)	(2×2)	1992		
		(110)	(2×2)	2007	2012	
		(111)	(2×2)	1981		
	RhBi	(100)	(2×2)	1964		
		(102)	(2×2)	1962, 1948		
		(110)	(2×2)	1973	1976	
	RhPb	(002)	(2×2)	1981	1984	
		(201)	(2×1)	1931		
		(211)	(2×1)	1956, 1939		
	$RhPb_2$	(100)	(2×2)	1982	1977	
		(001)	(2×1)	1993		
		(211)	(2×1)	1935		
bridge	Rh	(111)	(2×2)	1909	n. d.	1931[1]
	RhIn	(110)	(2×2)	1864	n. d.	
fcc hollow	Rh	(111)	(2×2)-3CO	1891	1880	1861[1]
gas phase				2143		2143[2]

[a] As-calculated values scaled by 1.0386 are reported as theoretical values. The scaling factor was determined as the ratio of the experimental and as-calculated values for gas phase CO.

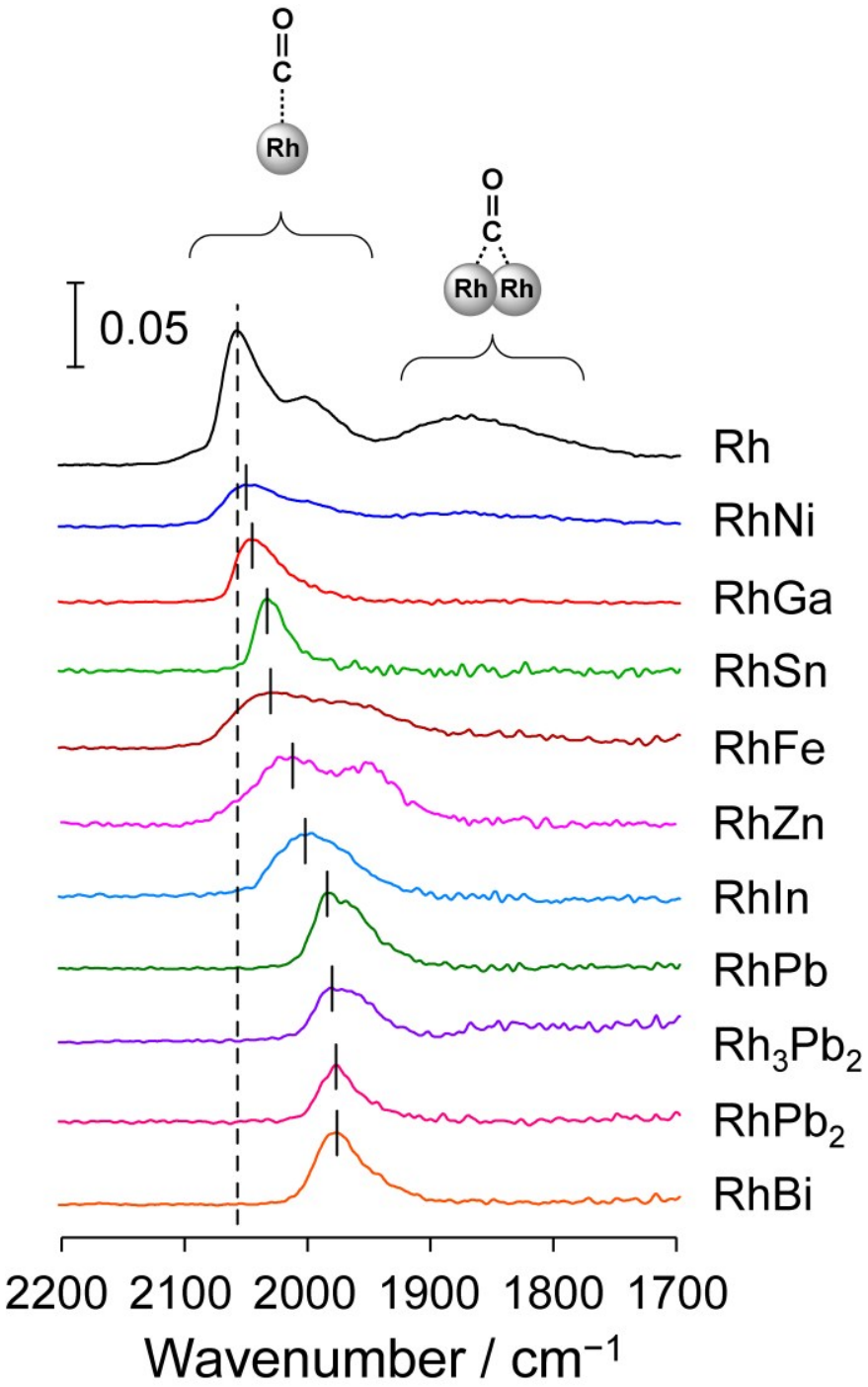

Figure S1. FT-IR spectra of CO adsorbed on Rh-based catalysts at 25°C. Vertical lines indicate the peak positions for linearly adsorbed CO. Spectra of which peak intensities are lower than 30% of those for saturation coverage are shown.

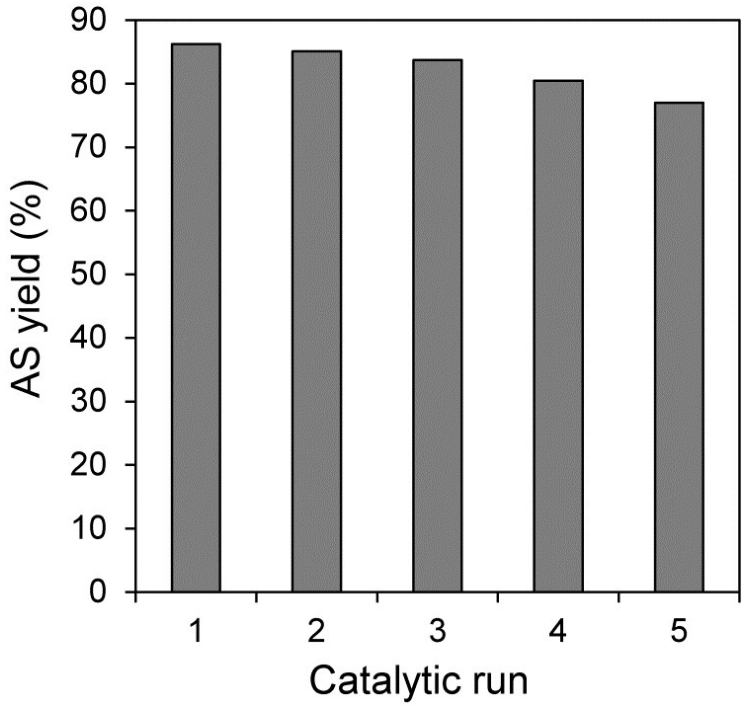

Figure S2. Reusability of $RhIn/SiO_2$ catalyst in NS hydrogenation at 75°C. To evaluate validly the change in catalytic performance, the reaction time was set to 1.5 h so that NS conversion at the first run did not saturate.

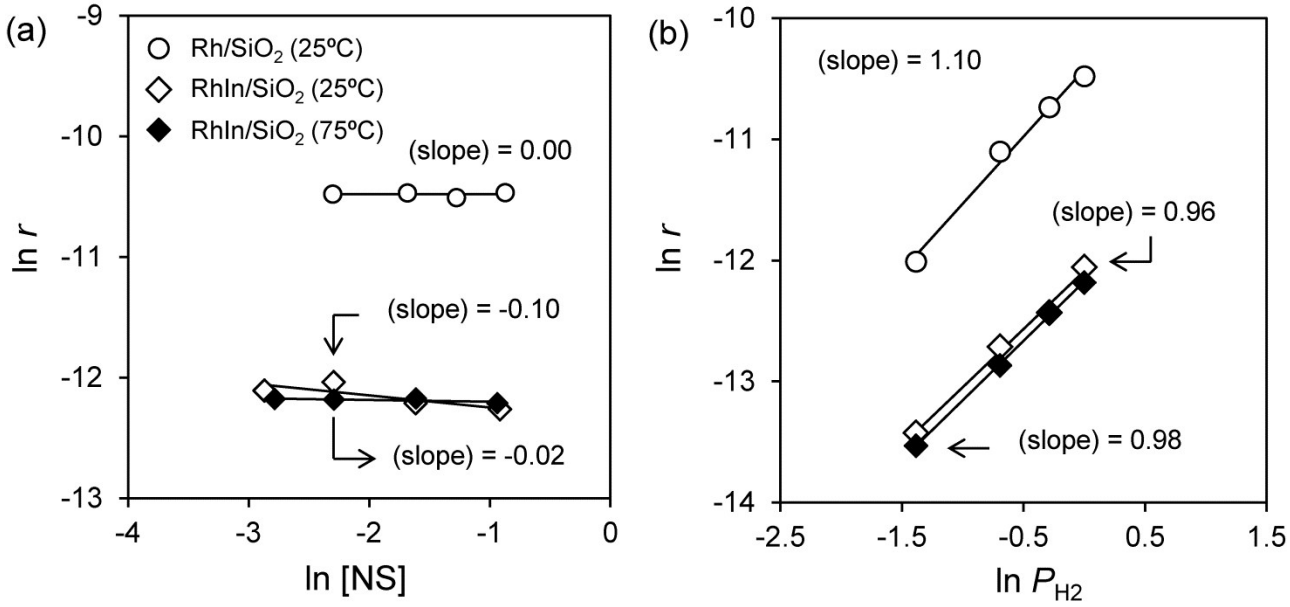

Figure S3. Dependences of reaction rate on (a) NS concentration and (b) H_2 pressure.

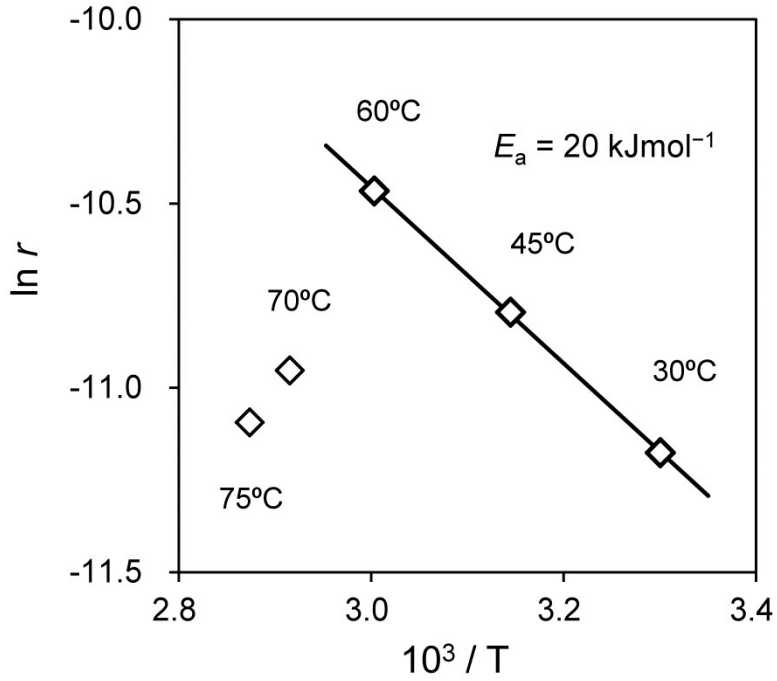

Figure S4. Arrhenius-type plot for NS hydrogenation over RhIn/SiO_2 under 1 atm H_2. The reaction condition was identical to that for Table 1.

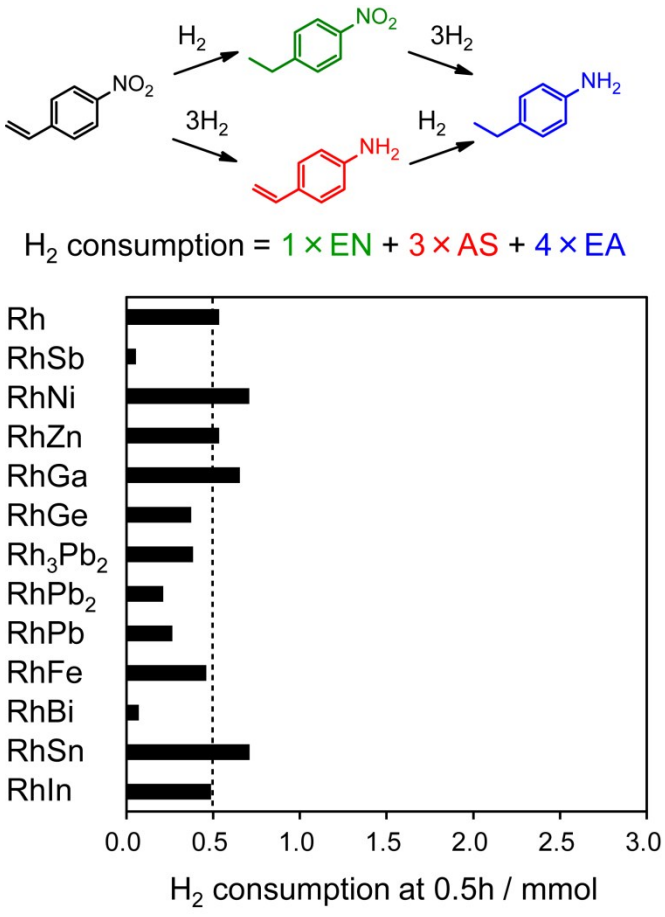

Figure S5. H_2 consumption at 0.5 h in NS hydrogenation over various Rh-based catalysts.

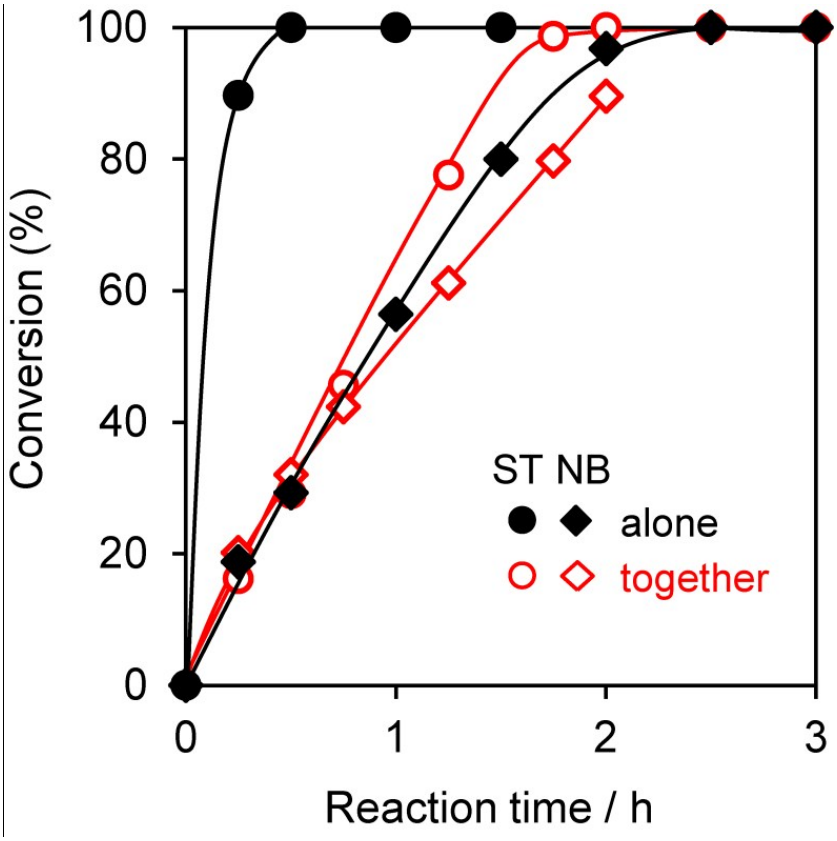

Figure S6. Time courses of ST and NB conversion when these substrates were used alone or together over $RhZn/SiO_2$. The reaction condition was identical to that for Table 1.

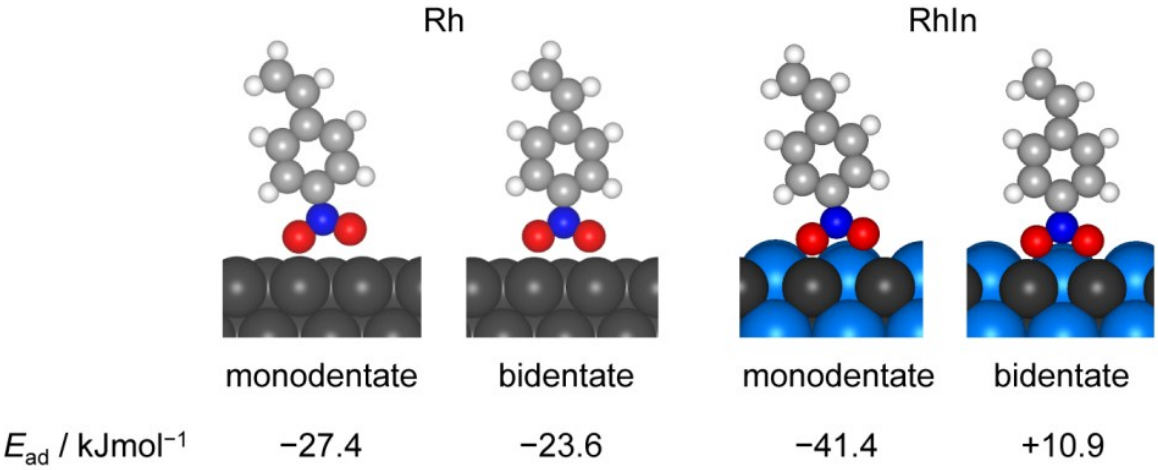

Figure S7. Optimized structures of NS adsorbed on Rh and RhIn with monodentate and bidentate ligation of the nitro group. The corresponding adsorption energies (E_{ad}) are also shown.

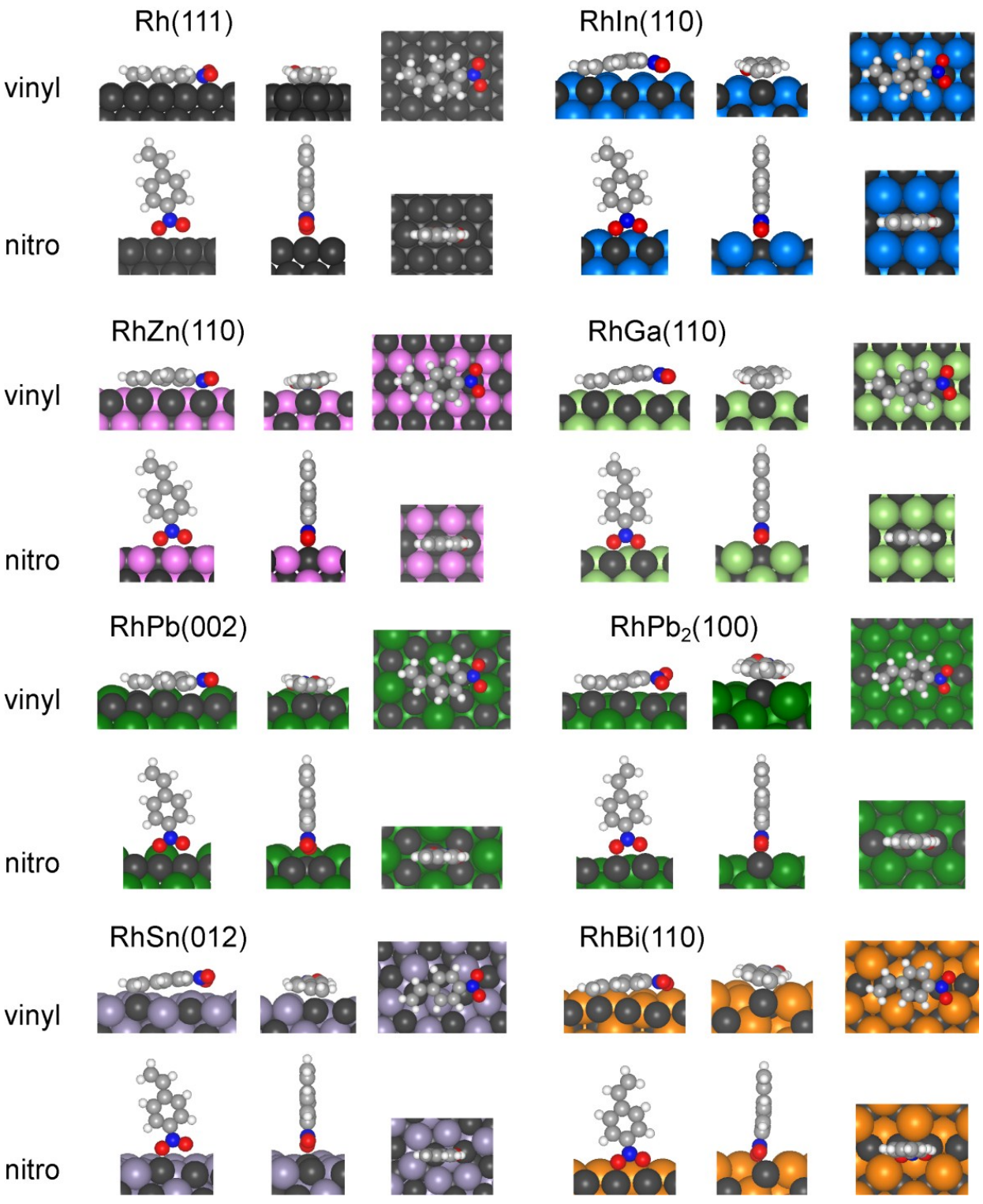

Figure S8. Optimized structures of NS adsorbed on varisou Rh-based materials.

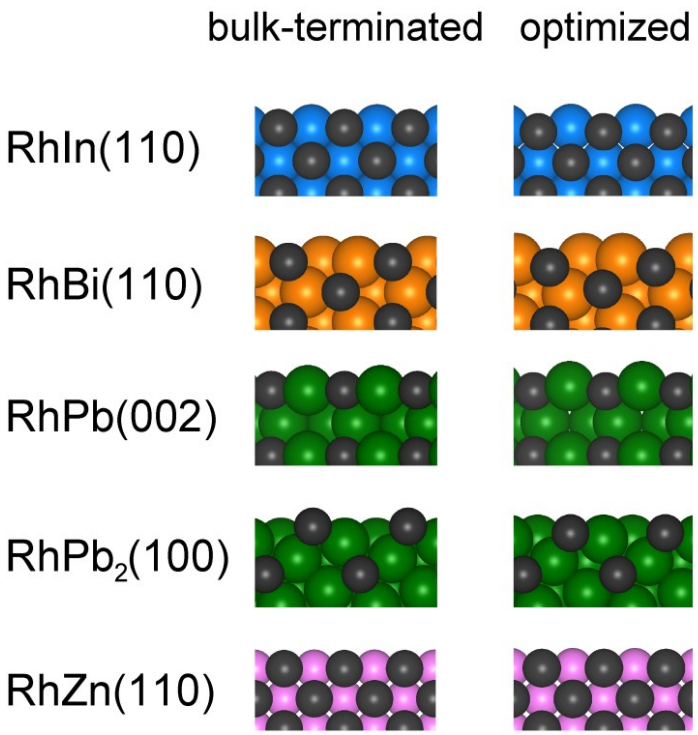

Figure S9. Bulk-terminated and optimized structures of several Rh-based planes.

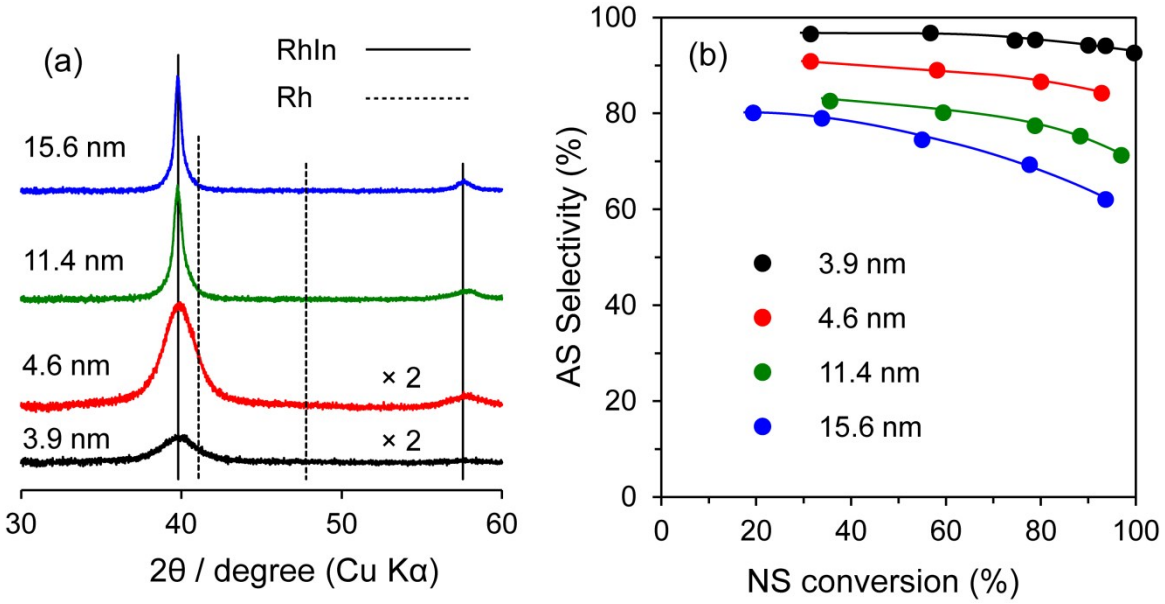

Figure S10. (a) XRD patterns of RhIn/SiO_2 with various crystallite sizes. (b) Conversion-selectivity curves obtained in NS hydrogenation using these RhIn/SiO_2 catalysts. The reaction condition is identical to that in the caption of Figure 3. RhIn(4.6) was obtained by annealing of RhIn(3.9) under He flow at 900°C for 1 h. RhIn(11.4) and RhIn(15.6) were prepared using parent Rh/SiO_2 with 6 and 9 nm of crystallite sizes, respectively. These Rh/SiO_2 were prepared without calcination and with reduction at 400°C and 600°C, respectively.

References

1. R. Linke, D. Curulla, M. J. P. Hopstaken and J. W. Niemantsverdriet, *J. Chem. Phys.*, 2001, **115**, 8209-8216.
2. D. Scarano, S. Bordiga, C. Lamberti, G. Spoto, G. Ricchiardi, A. Zecchina and C. O. Arean, *Surf. Sci.*, 1998, **411**, 272-285.